
Low-order models : optimal sampling and linearized control strategies

Edoardo Lombardi* — **Michel Bergmann****
Simone Camarri*** — **Angelo Iollo****

* *Optimad engineering srl*
10143 Torino, Italy
edoardo.lombardi@optimad.it

** *Institut de Mathématiques de Bordeaux and INRIA*
33405 Talence, France
michel.bergmann@math.u-bordeaux1.fr — angelo.iollo@math.u-bordeaux1.fr

*** *Dipartimento Ingegneria Aerospaziale, Università di Pisa*
36122 Pisa, Italy
s.camarri@ing.unipi.it

RÉSUMÉ. Nous proposons une méthode d'échantillonnage optimale pour construire un modèle d'ordre réduit basé sur la Décomposition Orthogonale aux valeurs Propres (POD) qui soit robuste par rapport à la variation des paramètres d'entrée. Cette méthode a été appliquée au cas de l'écoulement confiné autour d'un cylindre de section carré lorsque le nombre de Reynolds varie. Nous examinons également le lien entre les modes instables et la modélisation POD. Un exemple de contrôle basé sur une approche linearisée est présenté.

ABSTRACT. We propose an optimal sampling strategy to build a robust low-order model. This idea is applied to the construction of a vortex wake model accurate for several regimes. In addition we explore the relationships between unstable modes and low-order modelling. An example of control based on a linearized approach is presented.

MOTS-CLÉS : modèles réduits, échantillonnage optimal, contrôle

KEYWORDS: reduced order models, optimal sampling, control

1. Introduction

In fluid mechanics one of the most popular method to get a reduced-order model is the Proper Orthogonal Decomposition (POD) originally introduced in Lumley (1967) in turbulence context. The main drawback for flow control is that the POD basis is not optimal to represent a flow generated with different system parameters with respect to those used to build the basis. To get rid of this problem, different strategies can be employed. The first one is to update the POD basis as the system parameters change, as for instance in an iterative optimization problem. One method is to use trust region method (TRPOD see Bergmann *et al.* (2008a)), another is to calibrate over several dynamical cases (Weller *et al.*, 2009). Yet another method is to build a robust POD basis that can be used all along the optimization process. This kind of POD basis can be generated using chirp excitation (Bergmann *et al.*, 2005) or using an appropriate sampling of the input parameter space.

In this spirit, the first part of this study is devoted to the construction of a robust model that can be used for control without updating of the POD basis. The idea is to sample in an efficient way the input parameter subspace. Two classes of sampling methods are commonly used : the *one shot* method and the *iterative* one. In the *one shot* method the sampling is obtained by partitioning the range of variation of the input parameter space. The partitions can be found using different strategies as, for instance, the uniform distribution, the orthogonal sampling, the Sobol algorithm etc... An alternative strategy to the classical partition strategies is the Centroidal Voronoi Tessellations (CVT, see Du *et al.* (1999) and Burkardt *et al.* (2007)). The main idea of this method is to perform a partition of the space based on a density distribution. This kind of tessellations can be efficiently computed using the Lloyd algorithm (Du *et al.*, 2007). The main drawback of the *one shot* strategy is that the number of sampling points has to be fixed *a-priori* and, in the case of CVT, the final configuration is strongly dependent on the initial condition. Thus, an *a-priori* analysis of the density function used to compute the centroidal tessellation is necessary to determine the proper refinement when sampling the range of variation of the input parameter. The other class of methods (the iterative ones) consists in adding sampling points in an iterative way. The degree of accuracy can be chosen by fixing a stopping criterion. In greedy sampling (see Bui-Thanh *et al.* (2008)) the new value of the input parameter to sample is set at the maximum of the density function, *i.e.* where the error or the residual given by the POD basis is larger. In this study we propose a new approach that couples Constrained CVT and greedy methods.

In the second part of this study the control performance of a linearized low order model of the flow is assessed. In particular, a controller is designed by the low-order flow model which aims at stabilizing the otherwise unstable steady state of the system. To this purpose, a linear model is used, since it can model the small oscillations of the system around the target state. Indeed, designing the controller using a linear model involves standard techniques and is simpler than using a non-linear model. Moreover, it is also interesting to explore the capabilities of reduced-order models in estimating unstable modes in the linear stability analysis of a flow since this aspect is typically

very demanding in terms of computational costs. Indeed, this analysis requires codes simulating the linearized flow equations and, possibly, generating the matrix of the linearized system, which is not always possible when working with complex simulation codes as those typically used in engineering applications. Moreover, very large eigenvalue systems need to be solved. For this reason, the starting point of the present analysis is just the availability of a non-linear code for simulating the Navier-Stokes equations. The reduced order model of the linearized flow equations is built using only this tool. However, the use of a non-linear reduced-order model for flow control, although more expensive and complex, allows more general control strategies (*i.e.* minimization of general cost functions, different control targets etc...). In Weller *et al.* (2009) a control strategy based on a non-linear model is reported. In that reference it is also shown that their strategy, when used for the particular objective of stabilizing a steady state for the system, has a clear behavior in terms of the spectrum of the linearized Navier-Stokes operator around the target flow.

2. Flow configuration and POD strategies

In this study the two dimensional confined square cylinder wake flow (figure 1(a)) is chosen as a prototype of separated flow. The Navier-Stokes equations write :

$$\frac{\partial \mathbf{u}}{\partial t} + (\mathbf{u} \cdot \nabla) \mathbf{u} = -\nabla p + \frac{1}{Re} \Delta \mathbf{u} \quad [1a]$$

$$\nabla \cdot \mathbf{u} = 0 \quad [1b]$$

where $\mathbf{u} = (u, v)^T$ and p denote respectively the velocity and pressure fields. The parameter $Re = U_\infty L / \nu$ denotes the Reynolds number, with U_∞ the maximal inflow velocity of the incoming Poiseuille flow, L the length of the side of the square cylinder and ν the kinematic viscosity. We used the same numerical methods and parameters as those introduced in Galletti *et al.* (2004), *i.e.* the blockage ratio $\beta = L/H$ is equal to $1/8$ and the domain Ω is $(-10L, 22L) \times (-4L, 4L)$. For control purposes we placed two jets in opposite phase on the upper and lower faces of the cylinder, as shown in figure 1(b). Following the modeling of the actuators in Weller *et al.* (2008) and Weller *et al.* (2009) the boundary conditions on the jets areas Γ_c are :

$$v(\mathbf{x}, t) = c(t), \quad \mathbf{x} \in \Gamma_c$$

Without loss of generality we denote $\mathbf{U}(\mathbf{x}, t)$ the flow fields that can be for instance the velocity fields $\mathbf{u}(\mathbf{x}, t)$ or the pressure extended fields $(\mathbf{u}(\mathbf{x}, t), p(\mathbf{x}, t))^T$. The flow fields $\mathbf{U}(\mathbf{x}, t)$ can be approximated by :

$$\mathbf{U}(\mathbf{x}, t) \simeq \widehat{\mathbf{U}}^{[1, \dots, N_r]}(\mathbf{x}, t) = \sum_{n=1}^{N_r} a_n(t) \Phi_n(\mathbf{x}) + \mathbf{F}(\mathbf{x}, t) \quad [2]$$

where $\mathbf{F}(\mathbf{x}, t)$ can be any linear combinations of flow fields as the mean field $\overline{\mathbf{U}}(\mathbf{x})$, the unstable steady flow field $U_0(\mathbf{x})$, the control function with time de-

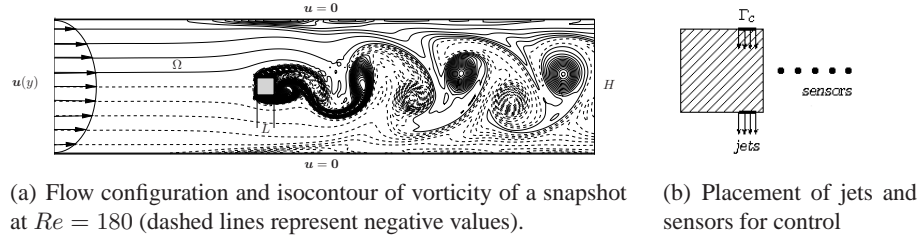


Figure 1. Sketch of the flow configuration with control actuation.

pendent actuation $c(t)U_c(\mathbf{x})$, or even zero. For both flow control strategies the basis functions $\Phi_n(\mathbf{x})$ are computed using the snapshot method introduced by Sirovich (Sirovich, 1987). The temporal coefficient $a_n(t)$ are solution of a reduced order model obtained by a Galerkin projection of the Navier-Stokes equation onto the POD basis functions.

3. POD ROM via efficient sampling of the input parameter space

The POD basis gives an optimal representation (in terms of kinetic energy when velocity fields $\mathbf{u}(\mathbf{x}, t)$ are used) of the snapshots database used to build the basis. However, the optimality of the basis is lost when the system changes due to a modification of its input parameters, as it is the case in control problems (see Prabhu *et al.* (2001) and Bergmann *et al.* (2008b)). The focus of this section is to improve the representation capabilities of a POD basis of a given flow when the Reynolds number varies in a given range $\mathcal{I} = [Re_L, Re_R]$, so as to provide a single ROM that is efficient for the considered range.

Numerically, we always considered a two dimensional laminar flow, *i.e.* $Re_R = 180$. Since the system undergoes the first Hopf bifurcation at $Re \approx 65$, we can consider both $Re_L = 70$ for periodic flows and $Re_L = 40$ to model the bifurcation. The interval \mathcal{I} is discretized with $\Delta Re = 5$, and it is denoted as \mathcal{I}_h . We will always use $N_r = 31$ basis functions so we simply denote $\tilde{\mathbf{U}}(\mathbf{x}, t) \equiv \tilde{\mathbf{U}}^{[1, \dots, N_r]}(\mathbf{x}, t)$ with $\mathbf{F} = \mathbf{0}$. We consider an initial database $U^{[Re_1, \dots, Re_N]}$ computed at N different Reynolds numbers. We take $N_s = 200$ snapshots at each Re_i . We want to improve the functional subspace enriching the database in a *one-shot* way by adding K sets of snapshots with $\{Re_i\}_{i=N+1}^{N+K} \in \mathcal{I}$. Let $M = N + K$ and $U^{[Re_1, \dots, Re_M]}$ be the database composed by M sets of snapshots taken at Re_1, \dots, Re_M . The three test cases presented in Fig. 2 are considered.

In what follows the sampling is performed according to an error estimator. As it will be explained later, we choose the L_2 norm of the Navier-Stokes residual as error estimator. It is thus necessary to approximate the pressure field. Following (Bergmann

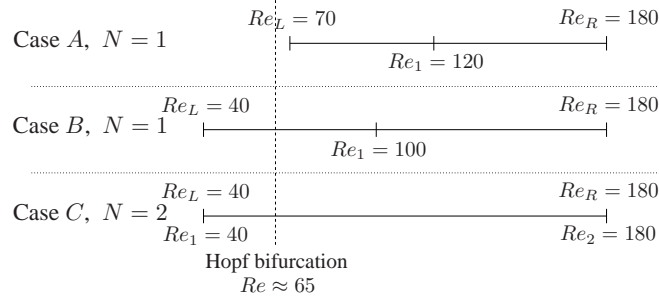


Figure 2. Sketch of the three test cases for sampling. The continuous horizontal line represents the range of Re that the POD database covers in each case.

et al., 2008b) the pressure term can be easily estimated by its POD ROM reconstruction \tilde{p} . The exact flow fields \mathbf{u} and p are then approximated by :

$$\tilde{\mathbf{u}}(\mathbf{x}, t) = \sum_{i=1}^{N_r} a_i(t) \phi_i(\mathbf{x}) \quad [3a]$$

$$\tilde{p}(\mathbf{x}, t) = \sum_{i=1}^{N_r} a_i(t) \psi_i(\mathbf{x}) \quad [3b]$$

A pressure extended reduced order model is obtained projecting the Navier-Stokes equations onto the POD basis functions $\Phi_i(\mathbf{x}) = (\phi_i(\mathbf{x}), \psi_i(\mathbf{x}))^T$. We use the same model as that derived in (Bergmann *et al.*, 2009), where we highlight the dependence versus the Reynolds number :

$$\sum_{j=1}^{N_r} L_{ij} \frac{da_j}{dt} = \frac{1}{Re} \sum_{j=1}^{N_r} B_{ij}^{Re} a_j + \sum_{j=1}^{N_r} B_{ij}^p a_j + \sum_{j=1}^{N_r} \sum_{k=1}^{N_r} C_{ijk} a_j a_k \quad [4]$$

with $B_{ij}^{Re} = -(\phi_i, \Delta \phi_j)_{\Omega}$ and $B_{ij}^p = +(\phi_i, \nabla \psi_j)_{\Omega}$ and an appropriate initial condition. The other model coefficients can be found in (Bergmann *et al.*, 2009). As discussed in several papers (Galletti *et al.*, 2006; Bergmann *et al.*, 2005; Couplet *et al.*, 2005), the initial value problem (4) can be inaccurate or even unstable. In order to build a robust order model we applied the calibration technique described in (Weller *et al.*, 2008).

In the following, the reconstruction capabilities of a given POD basis is evaluated when the Reynolds number varies in the interval $\mathcal{I} = [Re_L, Re_R]$. A natural way to achieve this is to compare, at each $Re \in \mathcal{I}_h$, the numerical solution $\mathbf{U}(\mathbf{x}, t)$ of the Navier-Stokes equations to the POD reconstruction $\tilde{\mathbf{U}}(\mathbf{x}, t)$ computed using a POD basis that corresponds to a given database $U^{[Re_1, \dots, Re_N]}$. Denoting $\mathbf{U}(\mathbf{x}, t)$ the numerical solution of the Navier-Stokes equations, the missing scales are

$$\mathbf{U}'(\mathbf{x}, t) = \mathbf{U}(\mathbf{x}, t) - \tilde{\mathbf{U}}(\mathbf{x}, t). \quad [5]$$

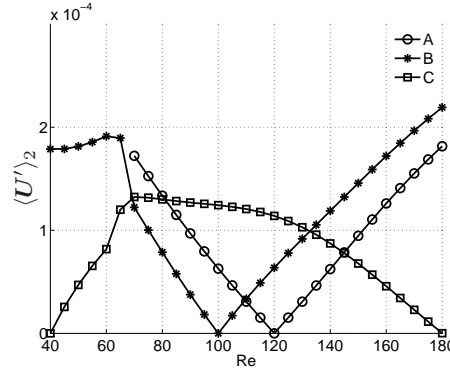


Figure 3. Evolution of the error $\langle U' \rangle_2$ versus the Reynolds number.

Let \mathbf{Y} be a vector belonging to the same subspace as the Navier-Stokes solution \mathbf{U} . We defined $\langle \mathbf{Y} \rangle_2$ the average of the L_2 norm over a temporal horizon T :

$$\langle \mathbf{Y} \rangle_2 = \int_T \frac{\|\mathbf{Y}(\mathbf{x}, t)\|_2}{T} dt. \quad [6]$$

The error $\langle U' \rangle_2$ indicates how the description capability of the POD basis changes due to variations of the Reynolds number. In what follows, the temporal horizon T is taken to be equal to three vortex shedding periods (that depends on Re). Figure 3 shows the evolution of the error $\langle U' \rangle_2$ versus the Reynolds number for the three initial databases under considerations. For all cases, we can see that the error is very small at Re_i , and then it grows when the value of the Reynolds number moves away from Re_i . This traduces the fact that the POD basis computed from a database collected from given dynamics is not able to give a good representation of flows that is characterized by other dynamics. The aim is then to determine a sampling $\{Re_i\}_{i=1}^N \in \mathcal{I}^N$, (with Re_1 fixed for all cases, plus Re_2 fixed for case C), to improve the robustness of the POD basis.

The evaluation of the error $U'(\mathbf{x}, t)$ is cpu demanding as it involves the computation of the numerical solutions $\mathbf{U}(\mathbf{x}, t)$ of the Navier-Stokes equations for each $Re \in \mathcal{I}_h$. It is then interesting to find an accurate estimation of the error [6]. To this end, we use the residuals of the Navier-Stokes operator, \mathcal{R} , evaluated using the POD ROM fields, $\tilde{\mathbf{U}}$. These residuals can be computed at low numerical costs. Indeed, we have to solve a POD ROM (very fast) and to compute its residuals.

A comparison between the error $\langle U' \rangle_2$ and its residuals based estimator $\langle \mathcal{R}(\tilde{\mathbf{U}}) \rangle_2$ over \mathcal{I}_h is performed in figure 4. It is interesting to note that these two quantities show a similar behavior for all the considered test cases. Indeed, the ratio $\langle \mathcal{R}(\tilde{\mathbf{U}}) \rangle_2 / \langle U' \rangle_2$ is approximately a constant over \mathcal{I}_h for all test cases. The residuals $\langle \mathcal{R}(\tilde{\mathbf{U}}) \rangle_2$ is thus a good estimator of the error $\langle U' \rangle_2$.

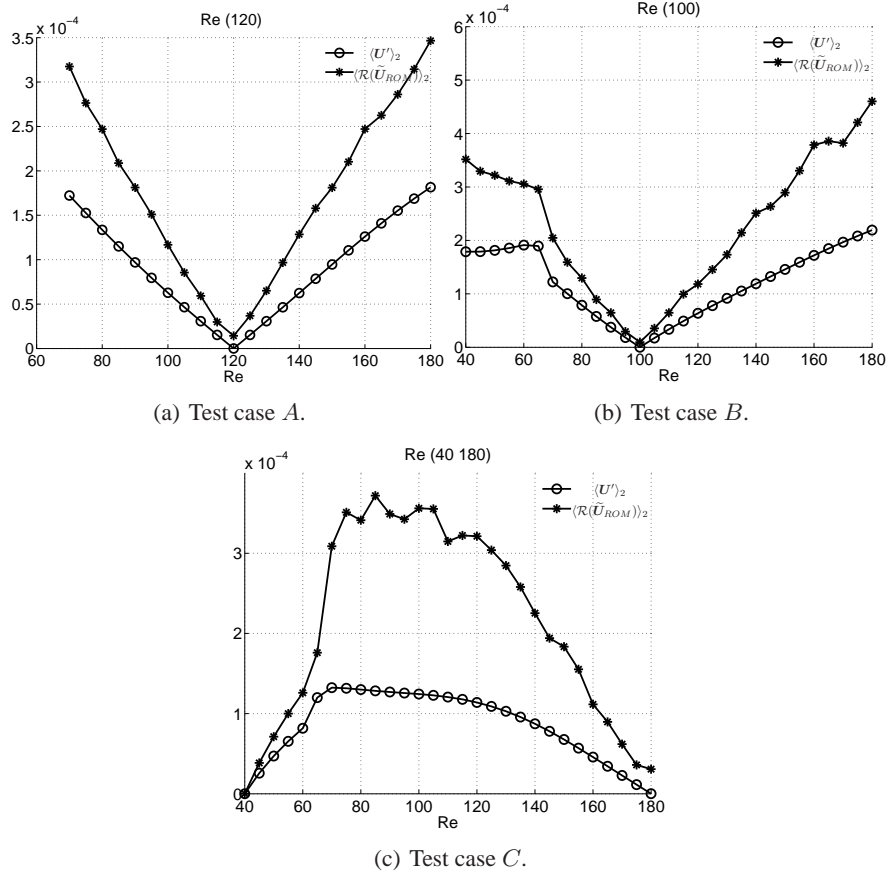


Figure 4. Comparison between the mean projection error $\langle U^I \rangle_2$ and the mean residuals $\langle \mathcal{R}(\tilde{U}_{DNS}) \rangle_2$ for the three test cases under consideration.

In this study we will present a *one shot* method based on greedy ideas (Bui-Thanh *et al.*, 2007). The density function is $\langle \mathcal{R}(\tilde{U}) \rangle_2$. Residuals $\mathcal{R}(\tilde{U})$ can be computed by integration of the calibrated ROM [4], built from initial database $U[Re_1, \dots, Re_N]$, for all Reynolds numbers in the discretized space $Re \in \mathcal{I}_h$. Since we want a robust POD basis, we look for a sampling $\{Re_i\}_{i=1}^M \in \mathcal{I}_h^M$ such that the database $U[Re_1, \dots, Re_M]$ produces models leading to reduction (or minimization in the optimal case) of the error evaluated over the whole subspace \mathcal{I}_h , where M has to be fixed as a function of the desired robustness.

We perform a Constrained Centroidal Voronoi Tessellation procedure (Du *et al.*, 2003) starting from a random subspace $Re_{z=z=N+1}^{M_0} \in \mathcal{I}_{M_0-N}$, with $M_0 > M$. The initial Reynolds numbers $[Re_1, \dots, Re_N]$ are frozen while the new points are

computed as being the centroids of the tessellation elements with respect to density function $\langle \mathcal{R}(\tilde{\mathbf{U}}) \rangle_2$. We exclude point $k > N$ with the smaller average density function over the k^{th} tessellation. This is done following greedy method in order to refine where the density function reaches higher values. The size of the sampling is then $M_1 = M_0 - 1$. This is an iterative process, and while $M_i > M$ we recompute a new Degenerated CCVT and exclude a new point $k > N$. The final configuration $M_i = M$ is weakly dependent on the initial configuration for $M_0 \gg M$. The main steps of the Greedy Degenerated CCVT are listed in the following, its final goal being the identification of a K -dimensional sampling to add at the N -dimensional initial sampling.

0. Random sampling with dimension $K_0 > K$. (the N first points are frozen).
- 1) At iteration i , start sampling process with dimension $M_i = K_i + N$
 - Perform a Constrained Centroidal Voronoi Tessellation
 - if $M_i = M$ stop
 - if $M_i > M$ go to 2
- 2) Identify and exclude point $k > N$ of the element with minimum integral
 - $M_{i+1} = M_i - 1$. Increment $i = i + 1$, then go to 1

The sampling method presented above can be easily transposed for input parameter subspaces with dimension greater than one. The use of the residuals as error estimation leads to negligible computational costs, even for high dimensional input parameter spaces, as for instance active control space.

In order to increase the robustness we chose to add $K = 2$ new sampling points in Re , with $K_0 = 6$ for the CCVT sampling method. Both CCVT and constrained uniform sampling CUS results restricted to \mathcal{I}_h are reported in table 1. The average

Test case	CCVT sampling	CUS sampling
<i>A</i>	{100, 55, 160}	{100, 70, 140}
<i>B</i>	{120, 80, 165}	{120, 90, 150}
<i>C</i>	{40, 180, 90, 130}	{40, 180, 85, 135}

Tableau 1. Sampling results with $K = 2$ for CCVT and CUS.

error and the standard deviation evaluated over the whole subspace \mathcal{I} are respectively defined by :

$$E = \frac{1}{Re_R - Re_L} \int_{\mathcal{I}} \langle \mathbf{U}'(Re) \rangle_2 dRe \quad [7]$$

$$R = \sqrt{\int_{\mathcal{I}} (\langle \mathbf{U}'(Re) \rangle_2 - E)^2 dRe}. \quad [8]$$

While the error E measures the accuracy of the POD ROM, the standard deviation R measures its robustness. These two quantities have been evaluated for the POD

models built using the sampling points found with both the Greedy Degenerated CCVT and the CUS strategies. For a scalar F we define a relative difference by $\Delta F = 100(F_{CUS} - F_{CCVT})/F_{CCVT}$. The CCVT sampling efficiency, ΔE , and robustness, ΔR , are reported in table 2. By definition, a positive difference means that CCVT is more efficient than CUS. Since ΔE and ΔR are always positive, CCVT reduced order models are more accurate and robust than the CUS ones. The CCVT ROM gives a good behaviour in terms of reconstruction error even in presence of a bifurcation. Thus, in a sampling procedure, one can use the Degenerated Greedy

A		B		C	
ΔE	ΔR	ΔE	ΔR	ΔE	ΔR
12.850	41.470	10.854	125.741	9.150	19.804

Tableau 2. CCVT sampling efficiency ΔE and robustness ΔR .

CCVT to build robust parameter dependent reduced order model. This avoids huge computational costs by using residuals estimation of the calibrated ROM instead of the approximation error computed by projection.

4. Control based on a linearized model

In this section the linearized reduced order model of the Navier-Stokes equations in presence of control actuation is described. The flow configuration is the same described in fig. 1. We consider a feedback proportional control actuated by the jets sketched in figure 1, using some measurements of vertical velocity given by N_v sensors placed at \mathbf{x}_j in the cylinder wake on the centre line. The control law with feedback gains K_j is :

$$c(t) = \sum_{j=1}^{N_v} K_j v(\mathbf{x}_j, t) \quad [9]$$

The aim is to find the set of feedback gains K_j that stabilizes the vortex shedding in the cylinder wake. The same problem on the same flow configuration has been solved in Camarri *et al.* (2010) without the use of reduced-order models.

The POD-based linear model is built using the snapshots obtained by a non-linear simulation of the transient flow dynamics, which is started from the steady unstable solution. The starting flow field, which is also the target flow of the controller, is found using the same code, by imposing the velocity field to be symmetric with respect to the symmetry line $y = 0$ and advancing the simulation in time until a steady state is reached.

Snapshots (N_s is their number) collected sampling a part of the transient dynamics, obtained with a particular control law $c(t)$, are used to build a POD model. To this purpose, every snapshot $\mathbf{u}(\mathbf{x}, t)$ is decomposed as follows :

$$\mathbf{w}(\mathbf{x}, t) = \mathbf{u}(\mathbf{x}, t) - \mathbf{u}_0(\mathbf{x}) + c(t)\mathbf{u}_c(\mathbf{x}) \quad [10]$$

where $\mathbf{u}_0(\mathbf{x})$ is the unstable steady state and $\mathbf{u}_c(\mathbf{x})$ is a flow field having a jet velocity equal to 1 and the velocity vanishing on all the other domain boundaries. This is obtained as proposed in Galletti *et al.* (2006).

Denoting $\{\phi_n\}_{n=1\dots N_r}$ the N_r retained modes obtained by applying the POD to $(\mathbf{w}(\mathbf{x}, t_i))_{i=1\dots N_s}$, the low-dimensional solution is written :

$$\tilde{\mathbf{u}}(\mathbf{x}, t) = \mathbf{u}_0(\mathbf{x}) + c(t)\mathbf{u}_c(\mathbf{x}) + \sum_{n=1}^{N_r} a_n(t)\phi_n(\mathbf{x}). \quad [11]$$

The Galerkin projection of the Navier Stokes equations onto the POD modes yields the same low order model derived in Weller *et al.* (2009).

The POD basis and the resulting model is built using the flow fields $\mathbf{w}(\mathbf{x}, t)$ (Eq. [10]) collected using different control laws which derive from different sets of feedback gains. The POD model is calibrated using all the simulations carried out to collect the snapshot database, and the conditioning of the calibration procedure is improved as proposed in Weller *et al.* (2009). Moreover, it is imposed that the steady unstable solution \mathbf{u}_0 is also a steady solution of the reduced order model and, consequently, the constant term is forced to vanish.

When the feedback control is found using the velocity field of the POD model, Eq. [9] becomes :

$$c(t) = \sum_{j=1}^{N_v} K_j v(\mathbf{x}_j, t) = \sum_{j=1}^{N_v} K_j \left(v_0(\mathbf{x}_j) + c(t)v_c(\mathbf{x}_j) + \sum_{r=1}^{N_r} \hat{a}_r(t)\phi_v^r(\mathbf{x}_j) \right) \quad [12]$$

where $\phi_v^r(\mathbf{x}_j)$ are the values of the component v of the POD modes at the sensors. Note that when steady unstable solution is used as target solution \mathbf{u}_0 , because of the symmetry, $v_0(\mathbf{x}_j) = 0$ and that $c(t)$ can be found in explicit form from Eq. ([12]) by trivial manipulation. In order to perform a stability analysis of the target state \mathbf{u}_0 and to perform an optimisation of the feedback control gains, the POD model is linearized around the equilibrium state $\mathbf{a}^* = 0$, (which corresponds to the flow field \mathbf{u}_0) and after algebraic manipulation, the low order model in matricial form becomes :

$$\begin{cases} \dot{\mathbf{a}}(t) &= \mathbf{L}(\mathbf{K}, \mathbf{x}_v)\mathbf{a}(t) \\ \mathbf{a}(0) &= \mathbf{a}^0 \end{cases} \quad [13]$$

where \mathbf{x}_v , the vector of the positions of the sensors, and \mathbf{K} , the set of feedback gains, are used as input parameters.

Since the system matrix \mathbf{L} of the linearized model depends explicitly on the feedback gains and on the position of the sensors, the model is predictive even when those parameters are changed with respect to the reference ones used for calibration. As already stated, the robustness of the model can be increased if, before linearization, a calibration procedure is used including several dynamics chosen by any sampling method, as detailed in Weller *et al.* (2008).

The linearized equation [13] can be used to perform a classical linear analysis of the dynamical system. Given the position of the sensors and the set of feedback gains \mathbf{K} , the stable/unstable eigenvalues of the system \mathbf{L} can be evaluated. For each eigenvalue, the associated eigenvector leads, by means of Eq. [10], to an estimation of the corresponding global mode of the linearized Navier-Stokes operator. A good accuracy on the estimation of the unstable modes of the full linearized Navier-Stokes problem allows to use the low order model in a control procedure, as described in the following. Note that the linearized reduced order model is obtained by using a simulation of a non-linear Navier-Stokes code. Moreover, the system matrix \mathbf{L} non-linearly depends on the feedback gains \mathbf{K} and on the position of the sensors \mathbf{x}_v , and this does not permit to use classical tools for the linear control. Thus, we propose here an iterative control procedure based on the minimisation of a functional cost, which is here after described.

As explained above, the accuracy of the linearized model is an important aspect, and this is briefly investigated in the following. As a first step, it is shown how to reconstruct a global mode associated to an eigenvector of the linearized POD system. The formal solution $\mathbf{a}(t)$ of the system [13] is :

$$\mathbf{a}(t) = \mathbf{R}e^{\mathbf{\Lambda}t}\mathbf{R}^{-1}\mathbf{a}^0 \quad [14]$$

where $\mathbf{\Lambda}$ is the diagonal matrix of the eigenvalues of \mathbf{L} , \mathbf{R} is the matrix whose columns are the corresponding eigenvectors and \mathbf{a}^0 is the initial condition on $\mathbf{a}(t)$. When Eq. [14] is substituted in Eq. [10], the fluctuating part of the velocity field $\tilde{\mathbf{u}}'(\mathbf{x}, t) = \mathbf{u}(\mathbf{x}, t) - \mathbf{u}_0(\mathbf{x})$ is obtained as follows :

$$\tilde{\mathbf{u}}'(\mathbf{x}, t) = \mathbf{Q}\mathbf{R}e^{\mathbf{\Lambda}t}\mathbf{R}^{-1}\mathbf{Q}^{-1}\tilde{\mathbf{u}}'(\mathbf{x}, 0) \quad [15]$$

with $\mathbf{Q} = (\mathbf{K}(\mathbf{I} - \mathbf{K}v_c(\mathbf{x}_v))^{-1}\phi_v(\mathbf{x}_v))$ and $\tilde{\mathbf{u}}'(\mathbf{x}, 0)$ the projection of the initial condition over the POD modes. Thus, assuming that the eigenvalues of the physical system are well approximated by the low order model, we can reconstruct the matrix containing physical eigenmodes $\mathbf{P} \approx \tilde{\mathbf{P}} = \mathbf{Q}\mathbf{R}$. In particular we are interested in the estimation of the unstable modes, which correspond to eigenvalues with positive real part.

In order to asses the accuracy of the feedback linear model described above, we consider a Reynolds number $Re = 85$, at which the instability is fully developed after a slow transient. In Figure 5 time evolution of the lift coefficient calculated on the cylinder with no control actuation is plotted. We recall that the simulation is carried

out by a non-linear Navier-Stokes code. Note the quick growth of the C_l after the slow transient regime. In the figure the portion of the transient used to build the POD model

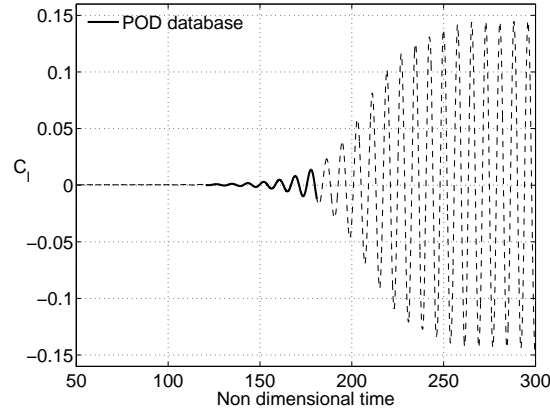


Figure 5. Lift coefficient C_l time evolution, with no control actuation at $Re = 85$.

is highlighted, using a continuous line. The interval is sampled considering $N_t = 250$ snapshots. This time interval is chosen starting when the lift coefficient reaches a value of $C_l \approx 0.001$ and including about seven quasi-periodic flow periods. We retain only $N_r = 6$ POD modes to build and calibrate the linearized low order model. This is motivated by the work documented in Galletti *et al.* (2006), where it is shown that a model similar to the one built here gives a good approximation of the unstable mode. Thus, the unstable mode estimated by the POD model can be analyzed to explore his observability and to consequently choose the position of the sensors for the feedback control. In particular we used only one sensor of vertical velocity, which is placed in

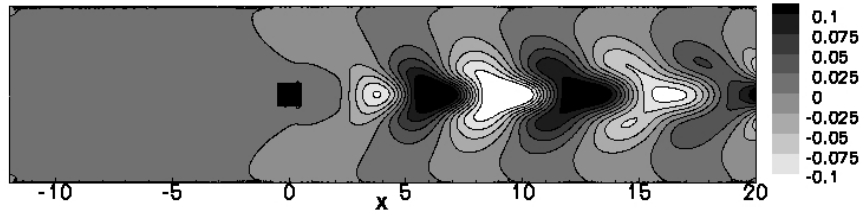


Figure 6. Reconstructed v -component of the physical unstable mode.

($x = 0.3, y = 0.0$), in the area of the first local minimum (maximum in terms of module) of the v -component of the unstable mode (see figure 6). In order to test the capability of the feedback linear low order model to estimate the physical unstable mode in the presence of an actuation, we performed two numerical simulations of the actuated flow using two different proportional feedback gains for the sensor placed

as described above, *i.e.* $k = 0.1$ and $k = 0.2$. As in the previous case, the two time intervals used to build the model include seven flow oscillations starting from a value of $C_l \approx 0.001$, with $N_t = 250$ snapshots for each case.

As expected, only two unstable conjugate eigenvalues are predicted by the linear low order model, and the estimation of the unstable eigenvalues given by reduced model is very accurate. The percentage error on the estimation of the real and the imaginary part of the unstable eigenvalues are respectively 7.62% and 0.26% when $k = 0.1$ is used and 0.11% and 0.12% for $k = 0.2$. In figure 7 the module of the

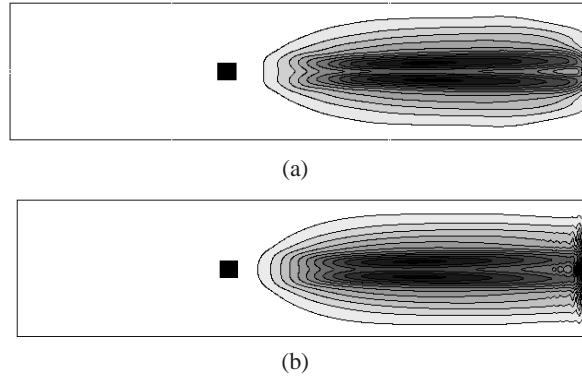


Figure 7. Isocontour of the module of the predicted (a) and the physical (b) unstable eigenmode for the case $k = 0.2$. Plots obtained with the same scale level.

reconstructed unstable mode for the case $k = 0.2$ and the one found by a linearized analysis of the Navier-Stokes operator are plotted. The prediction of the mode is very accurate in the whole domain ; only a slight difference can be noted at the outflow due to the influence of the imposed boundary conditions in the linearized Navier-Stokes code. An analogous result is obtained in the case $k = 0.1$.

In order to stabilize the steady state, the unstable eigenvalues need to be moved in the stable region of the complex plane. To this aim, while the position of the sensors are kept constant, a function of the gains \mathbf{K} is proposed, such that its minimisation is equivalent to stabilize the system :

$$\mathcal{F}(\mathbf{K}) = \sum_{r=1}^{N_r} \tanh(\text{Re}(\lambda_r(\mathbf{K})) - \lambda_{Re}^*) + \alpha_K \min_{l=1, \dots, N_c} ((\mathbf{K} - \mathbf{K}_l^0)^2) \quad [16]$$

where λ_r are all the N_r eigenvalues predicted by the linear feedback model as \mathbf{K} varies, λ_{Re}^* is the stability margin required, \mathbf{K}_l^0 is the set of $l - th$ gains used to build the model and the parameter, $\alpha_K \ll 1$ has to be chosen as a measure of the trust region of the low order model. In our application we use $\alpha = 0.1$. The function $\tanh(\cdot)$ is chosen to retain the position of the eigenvalues already stable with the margin sufficiently larger than λ_{Re}^* , while the other eigenvalues are modified.

The minimisation gives an optimal set of parameters \mathbf{K}^* for the present model. This set of gains are tested in a non-linear Navier-Stokes simulation after the impulsive start of the flow. If the target state is not stabilized a new reduced order model is built with a database obtained by adding a portion of the transient of the new dynamics to the old POD database. During the optimisation procedure a maximum number of dynamics in the POD database can be fixed *a priori*, then when the maximum number is reached, a new set of snapshots substitutes the one with maximum distance $|\mathbf{K} - \mathbf{K}^*|$. Again, a minimisation of the functional [16] is carried out and a new set of parameters are obtained. The procedure is stopped when the steady state is stabilized.

In the test described here, the model built using the databases obtained with $k = 0.1$ and $k = 0.2$ is initially used for the optimization. The minimisation of [16] gives a new value of the feedback gain $k^* = 0.44$. A non-linear simulation of the Navier-Stokes equations starting from \mathbf{U}^0 is carried out, and the resulted flow is completely stabilized, as shown in figure 8 and 9. In figure 8 the lift coefficients obtained with $k = 0.1$, $k = 0.2$ and k^* are plotted. The use of the optimised feedback gain leads to

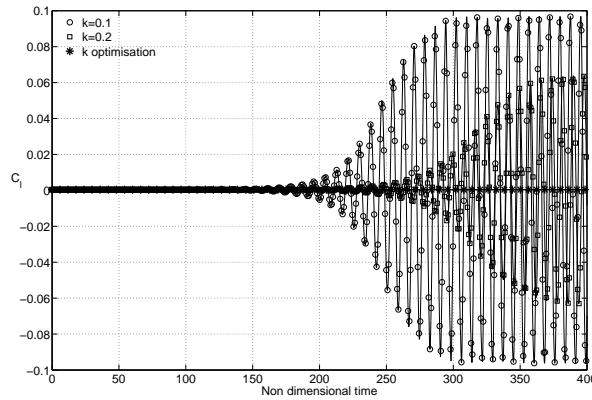


Figure 8. Lift coefficient obtained with $k = 0.1$, $k = 0.2$ and $k^* = 0.44$. Sensor position $(0.3,0.0)$ and $Re = 85$.

a steady and vanishing lift coefficient. Thus, the flow is totally controlled as displayed in figure 9, where the vorticity field of the flow obtained with k^* at time $t = 480$ is shown.

Finally, the reduced order model obtained by a non-linear Navier-Stokes code and successively linearized around a steady state, is able to represent, with limited computational costs, the unstable modes of the linearized Navier-Stokes operator, and a control optimisation based on such a linearized model gives a set of input parameters that stabilizes the actual flow. We recall that the whole procedure can be performed starting from the simulations of a generic non-linear code as those typically used in engineering applications.

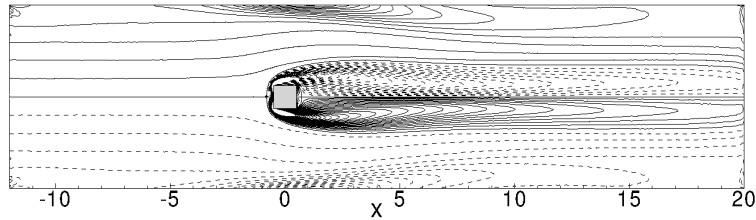


Figure 9. Vorticity snapshot of controlled flow with $k^* = 0.44$ at time $t = 480$.

The obtained results allow us to use the optimisation based on the linear feedback low order model in a control procedure for flow at higher Reynolds numbers and with a higher number of sensors. The main difficulty is to build a POD model which is robust with the parameters variation. Indeed the most significant computational cost of the procedure is the update of the linear model, which needs new DNS simulations. A more robust model is characterized by a wider trust region and needs a reduced number of updates to complete the optimization. For this reason, the goal of future works is to couple the two techniques described in this study, *i.e.* to build a robust low order model to be used in the linearized control design strategy.

5. Bibliographie

- Bergmann M., Bruneau C., Iollo A., « Enablers for robust POD models », *J. Comput. Phys.*, vol. 228, n° 2, p. 516-538, 2009.
- Bergmann M., Cordier L., « Optimal control of the cylinder wake in the laminar regime by trust-region methods and POD reduced-order models », *J. Comput. Phys.*, vol. 227, n° 16, p. 7813-7840, 2008a.
- Bergmann M., Cordier L., « Optimal control of the cylinder wake in the laminar regime by Trust-Region methods and POD Reduced-Order Models », *J. Comp. Phys.*, vol. 227, n° 16, p. 7813-7840, 2008b.
- Bergmann M., Cordier L., J.-P.Brancher, « Optimal rotary control of the cylinder wake using proper orthogonal decomposition reduced-order model », *Physics of Fluids*, vol. 17, p. 097101, 2005.
- Bui-Thanh T., Willcox K., Ghattas O., *Parametric reduced-order models for probabilistic analysis of unsteady aerodynamic applications*, Collection of Technical Papers, Vol. 4, AIAA/ASME/ASCE/AHS/ASC, 2007.
- Bui-Thanh T., Willcox K., Ghattas O., « Model reduction for large-scale systems with high-dimensional parametric input space », *SIAM J. Sci Comp*, 2008. In press.
- Burkardt J., Gunzburger M. D., Lee H.-C., « Centroidal Voronoi Tessellation-Based Reduced-Order Modeling of Complex Systems », *SIAM J. Sci Comp*, vol. 28, n° 2, p. 459-484, 2007.
- Camarri S., Iollo A., « Feedback control of the vortex-shedding instability based on sensitivity analysis », *Phys. Fluids*, vol. 22, n° 9, p. 094102, 2010.

- Couplet M., Basdevant C., Sagaut P., « Calibrated reduced-order POD-Galerkin system for fluid flow modelling », *J. Comput. Phys.*, vol. 207, n° 1, p. 192-220, 2005.
- Du Q., Emelianenko M., Ju L., « Convergence of the lloyd algorithm for computing centroidal Voronoi tessellations », *SIAM journal on numerical analysis*, vol. 44, n° 1, p. 102-119, 2007.
- Du Q., Faber V., Gunzburger M. D., « Centroidal Voronoi tessellations : Applications and algorithms », *SIAM Review*, vol. 41, n° 4, p. 637-676, 1999.
- Du Q., Gunzburger M. D., Ju L., « Constrained Centroidal Voronoi Tessellations for Surfaces », *SIAM Journal on Scientific Computing*, vol. 24, n° 5, p. 1488-1506, 2003.
- Galletti B., Bottaro A., Bruneau C., Iollo A., « Accurate model reduction of transient and forced flows », *Europ. J. Mech. / B Fluids*, vol. 26, p. 354-366, 2006.
- Galletti B., Bruneau C. H., Zannetti L., Iollo A., « Low-order modelling of laminar flow regimes past a confined square cylinder », *J.Fluid Mech.*, vol. 503, p. 161-170, 2004.
- Lumley J. L., « The Structure of Inhomogeneous Turbulent Flows », In *Atmospheric Turbulence and Radio Wave Propagation*, edited by A. M. Yaglom and V. L. Tatarski, Nauka, Moscow, vol. , p. 166-178, 1967.
- Prabhu R. D., Collis S. S., Chang Y., « The influence of control on Proper Orthogonal Decomposition of wall-bounded turbulent flows », *Phys. Fluids*, vol. 13, n° 2, p. 520-537, 2001.
- Sirovich L., « Turbulence and the dynamics of coherent structures. Parts I,II and III », *Quarterly of Applied Mathematics*, vol. XLV, p. 561-590, 1987.
- Weller J., Camarri S., Iollo A., « Feedback flow control design by low-order modeling for laminar wake stabilization », *Journal of Fluid Mechanics*, vol. 634, p. 405-418, 2009.
- Weller J., Lombardi E., Iollo A., « Robust model identification of actuated vortex wakes », *Physica D : nonlinear phenomena*, vol. 238, p. 416-427, 2008.